

Electrochemical polymerization of neutral red in the presence of sulfoferrocenecarboxylic acid

Chuanxiang Chen*, Yuhua Gao

*Department of Chemistry, School of Materials Science and Engineering,
Jiangsu University Science and Technology, Zhenjiang 212003, People's Republic of China*

Received 23 December 2006; received in revised form 8 May 2007; accepted 29 June 2007
Available online 15 July 2007

Abstract

Syntheses, properties and applications of polyaniline and its derivatives have been studied extensively. Recent papers have shown that their micro-structures can be prepared using chemical, electrochemical and physical methods. Here, we describe oxidative polymerization of neutral red, an aniline derivative, carried out in aqueous sulfuric acid solution containing sulfoferrocenecarboxylic acid using repeated potential cycling. The polymer film was electrochemically deposited on a platinum anode and had an electrochemical activity in the solution of 0.5 mol dm^{-3} Na_2SO_4 with $\text{pH} \leq 7.0$. Based on the spectroscopic measurements, a possible chemical structure of the corresponding polymer was proposed. The scanning electron microscopy micrograph proved that the micro-structure of the resulting polymer, which portrayed geological features similar to Earth and Titan, can be prepared using the electrochemical method.

© 2007 Elsevier Ltd. All rights reserved.

Keywords: Electroactive polymer; Oxidative coupling polymerization; Morphology

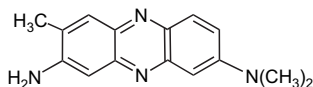
1. Introduction

Conducting polymers have been attracting significant interest due to their useful physical and chemical properties, including electronic, electrochemical and optical ones. Electrochemical studies will help us understand the relationship between the structure and property of each conducting polymer. These studies are of utmost important in developing novel conducting polymer materials and their electrochemical devices. Among these polymers, poly(neutral red) may be promising in view of its properties possessing both monomer and polymer types of redox behavior [1,2]. Neutral red (Scheme 1) is a redox indicator and mediator in various branches of biochemistry and bioelectrochemistry [2]. Neutral red and its

polymer have been used in chemically modified electrodes, and the electrode processes of these chemically modified electrodes have been investigated extensively [2–15]. It is noted that electropolymerizations of neutral red have been studied mainly in weak acidic, neutral and basic solutions [2], while there were few studies concerning the oxidative polymerization of neutral red in strong acidic solutions [7,14,15].

Incorporation of metallic particles into conducting polymers increases specific area of these polymer materials [16–18]. Ferrocenyl derivatives and polymers containing ferrocene have been used in chemically modified electrodes due to their unique redox electrical, magnetic and other characteristics [19–25]. Pournaghi-Azar and Ojani [26] investigated the electrosyntheses of polypyrrole incorporated ferrocenecarboxylic acid and its electrocatalytic oxidation of ascorbic acid. Yamamoto et al. [27] reported that acid doping of ferrocenesulfonic acid as a dopant in polyaniline took place homogeneously, and the resulting polyaniline had high conductivity since the dopant was incorporated at ca. 100% efficiency (dopant/polyaniline 2 units). They thought that the doping reaction

* Corresponding author. Tel.: +86 511 4401181; fax: +86 511 4407381.
E-mail address: cxchenyz@yahoo.com.cn (C. Chen).



Scheme 1. Chemical structure of neutral red.

was dominated by diffusion kinetics. Mu and coworkers [28–34] extensively studied the electrochemical activity and catalytic effect of polyaniline doped with ferrocenesulfonic acid which are much better than those of normal polyaniline. Li et al. [35,36] investigated polynaphthylamine that was electrosynthesized in the presence of ferrocenesulfonic acid and was used as a modified electrode. They reported that the electrochemical activity and catalytic behavior of the resulting polynaphthylamine were improved by the above synthesis method. Ndamanisha et al. [37] recently discussed the electrochemical preparation of polyaniline doped with sulfoferrocenecarboxylic acid (SFCA) and its application to the electrocatalytic oxidation of methanol. However, to date, there are no reports in the literature on the effect of SFCA on the electropolymerization of neutral red, an aniline derivative, and the characteristics of the resulting polymer. In the present work, we present the mechanistic investigations of the electropolymerization of neutral red in the presence of SFCA, and electrochemical activity, scanning electron microscopy (SEM), visible spectrum, infrared spectrum (IR) and X-ray photoelectron spectroscopy (XPS) of the resulting polymer.

2. Experimental

The purity of ferrocenecarboxylic acid was higher than 99% and was used without further purification. SFCA was prepared via the chemical reaction according to the procedure in the literature [37]. All other chemicals were of analytical-reagent grade and were used as received. Doubly distilled water was used to prepare solutions.

Electrochemistry was performed with a HPD-1A potentiostat–galvanostat and a YEW model 3086 X–Y recorder. Cyclic voltammetry was conducted with the use of a typical three-electrode cell. Two platinum foil electrodes were used as the working electrode and auxiliary electrode, respectively. The area of a platinum foil was $7 \times 2 \text{ mm}^2$. All cell potentials were measured with respect to the saturated calomel reference electrode (SCE) and all potentials are reported with respect to the SCE. The scan rate of 60 mV s^{-1} was applied for all electrochemical experiments, unless otherwise stated. The temperature for the electrochemical experiments was controlled at 30°C .

The oxidative polymerization of neutral red was carried out by cyclic voltammetry in a solution consisting of 5.0 mmol dm^{-3} neutral red, 0.15 mol dm^{-3} SFCA and 0.50 mol dm^{-3} H_2SO_4 . To prove the attribution of the redox peaks in the i – E curves of the resulting polymer, one separate cyclic voltammetry was carried out in 5.0 mmol dm^{-3} neutral red and 0.50 mol dm^{-3} H_2SO_4 , and another separate cyclic voltammetry was carried out in 0.15 mol dm^{-3} SFCA and

0.50 mol dm^{-3} H_2SO_4 . The sweeping potential range was set in a range of -0.20 to 1.20 V for the above three experiments. The electrochemical properties of the resulting polymer film were analysed in various pH aqueous Na_2SO_4 solutions. The pH values of the solutions were measured with a PXD-12 meter. The pH values of the solution were adjusted with a solution of NaOH or a solution of H_2SO_4 , depending on the pH value.

Visible spectra of neutral red and the corresponding polymer film were obtained with a Hitachi model U-3010 UV–vis spectrophotometer. The ex situ reflection–absorption IR spectrum of the polymer film was recorded, using a bare platinum surface as reference, on a Digilab model FTS 2000 Fourier transform-infrared spectrometer. The interference fringes observed in the original spectra were mostly eliminated through special spectral subtraction. The XPS investigations were performed with a Thermo VG Scientific Escalab 250 system equipped with a hemispherical analyzer and an Al anode ($K\alpha$ X-rays at 1486.6) used at 10 kV and ca. 15 mA . The binding energies were corrected for surface charging by referencing to C 1s neutral carbon peak at 284.6 eV . The morphology of the deposited polymer film was observed using SEM on a JEOL model JSM-6480 microscope.

3. Results and discussion

3.1. Electropolymerizations of NR

Fig. 1A shows the cyclic voltammograms of poly(neutral red) film growth during the electrolysis of a solution containing 5.0 mmol dm^{-3} neutral red and 0.50 mol dm^{-3} H_2SO_4 . There are two anodic peaks at -0.04 and 0.95 V and a cathodic peak at -0.09 V for the first cycle (curve 1). The anodic peak at ca. 0.95 V corresponds to the formation of the radical cation dye. The anodic peak current at about -0.04 V and the corresponding cathodic peak current at ca. -0.09 V increase with the number of potential cycles, indicating a successive increase in the amount of the poly(neutral red) film. This result is similar to the general electropolymerization of neutral red from solutions with pH close to neutral [2]. The poly(neutral red) obtained here is expressed as PNR.

Fig. 1B and C are the cyclic voltammograms of the electropolymerization of neutral red from a solution consisting of 5.0 mmol dm^{-3} neutral red, 0.15 mol dm^{-3} SFCA and 0.50 mol dm^{-3} H_2SO_4 . As shown in Fig. 1B, two redox couples appear in the first cycle (curve 1). One takes place at about 0.40 V , and the other occurs at ca. 0.70 V . From the second cycle to the seventh one, both the redox couples appear but decrease. In the eighth cycle, a new anodic peak (shoulder) appears around 0.95 V . The new anodic peak is also observed but is shifted slightly towards higher positive values and becomes more pronounced in the ninth and subsequent cycles. This reason is due to both the low conductivity of the resulting polymer film which is growing during the electrolysis process being lower than that of the Pt foil electrode and there are changes of pH at the electrode surface during electrolysis. Moreover, the new anodic peak current becomes more pronounced from the 12th and subsequent cycles in comparison

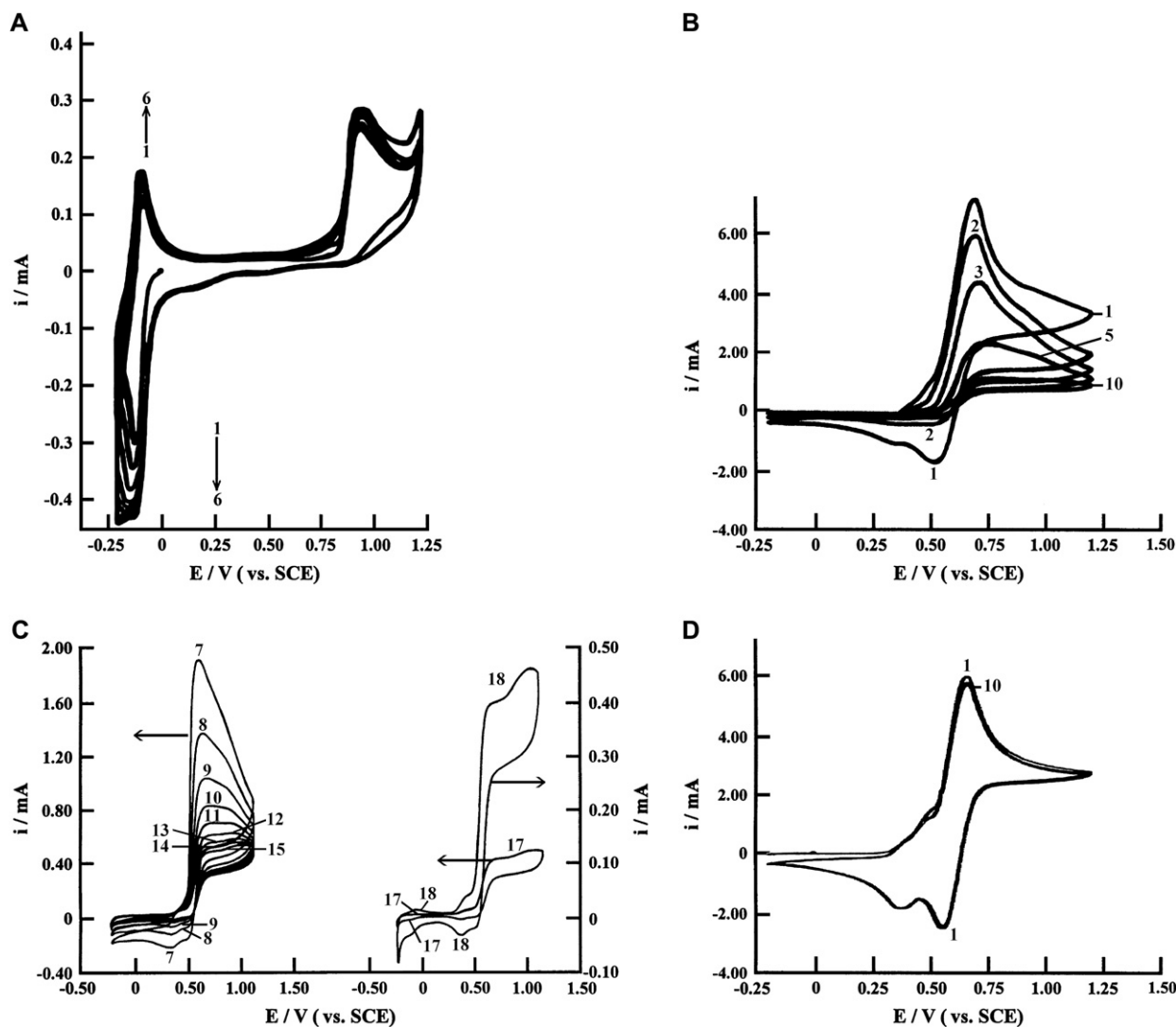


Fig. 1. Cyclic voltammograms of electrolysis of $0.5 \text{ mol dm}^{-3} \text{ H}_2\text{SO}_4$ solutions containing 5 mmol dm^{-3} neutral red (A), 5 mmol dm^{-3} neutral red in the presence of 0.15 mol dm^{-3} SFCA (B and C) and 0.15 mol dm^{-3} SFCA in the absence of neutral red (D). Scan rate: 60 mV s^{-1} . The number of curves in the plot corresponds to the number of cycles.

with the anodic peak of the redox couple at ca. 0.70 V . In addition, a redox couple at ca. -0.10 V also becomes more pronounced during electrolysis, while each of the two redox couples around 0.40 and 0.70 V , respectively, appears weaker from the second cycle to the 18th one. This reason was also due to the film thickness of the resulting polymer on platinum gradually growing during the electrolysis process. Indeed the redox couple at about -0.10 V occurs from the first cycle. The redox couple at ca. -0.10 V is attributed both to the reduction/reoxidation of the polymer film and to the overlapping of the neutral red monomer [6,14].

Besides the $i-E$ curves in Fig. 1C are different in shapes from those in Fig. 1A for the same cycle, the peak areas in Fig. 1C are larger than those in Fig. 1A for the same cycle, indicating SFCA in the neutral red solution can accelerate the electropolymerization of neutral red. The reason for this is that SFCA plays an important role in electron transfer. After electrolysis, a red film was observed on the working electrode.

The poly(neutral red) synthesized in the presence of SFCA is expressed as PNR-SFCA.

As mentioned above, the peak currents of the two redox couples at ca. 0.40 and 0.70 V , respectively, decrease with the number of potential cycles in Fig. 1B and C. In order to prove the attribution of the two redox couples, the $i-E$ curves of SFCA are used (Fig. 1D). As seen in Fig. 1D, one of two redox couples takes place at ca. 0.40 V , and the other occurs at ca. 0.70 V , but their peak currents are all independent of the number of potential cycles except for the first one. Thus, the two corresponding redox couples in Fig. 1B and C should be attributed to the redox of SFCA itself. It is noted that the changes in the peak currents of the two redox couples in Fig. 1B and C with the number of potential cycles are also caused by the film thickness of the resulting polymer deposited onto the working electrode.

According to the procedure in the literature [37], the PNR-SFCA film was purified. This purification of the resulting

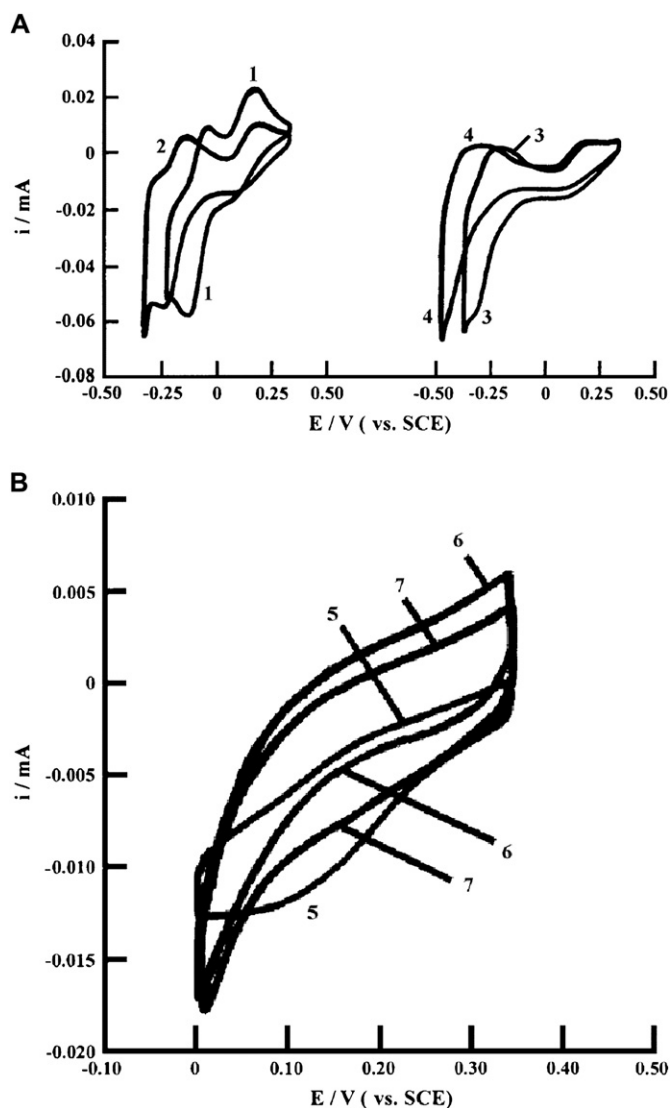


Fig. 2. Effect of pH value on the cyclic voltammograms of PNR-SFCA in $0.5 \text{ mol dm}^{-3} \text{ Na}_2\text{SO}_4$ solution. Scan rate: 60 mV s^{-1} . The number of curves in the plot corresponds to the pH values.

polymer is enough to evaluate its electrochemical properties and structure.

3.2. Effect of pH on the cyclic voltammograms of PNR-SFCA

Fig. 2 displays the cyclic voltammograms of PNR-SFCA in $0.5 \text{ mol dm}^{-3} \text{ Na}_2\text{SO}_4$ solutions with various pH values. As seen on curve 1, a main redox peak (the first wave) appears at about -0.07 V . This redox peak is shifted towards more negative potentials when pH value increases from 1.0 to 4.0. The cathodic and anodic peak potentials are dependent on the slopes of -100 ± 5 and $-101 \pm 5 \text{ mV/pH}$ (Fig. 3), respectively, indicating that the redox peak of PNR-SFCA is a $1\text{e}^-/2\text{H}^+$ reaction, which is close to that given by the Nernstian equation [38]. At less acidic solutions, the redox process of the polymer at a negative potential is related to proton concentration of the solution, i.e.

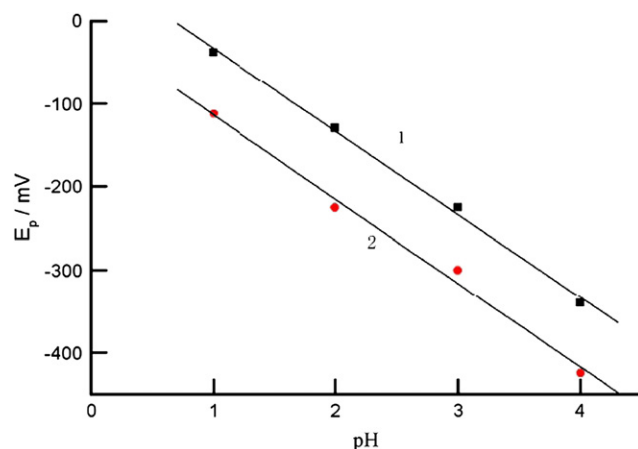


Fig. 3. Redox peak potential values vs. pH based on Fig. 2A. Curves: (1) anodic peak, (2) cathodic peak suited at negative potentials.

protons in the polymer enter into the solution for the oxidation process, and vice versa for the reduction process. This property is very similar to that of polyaniline [39]. It was also observed that the cathodic peak current (i_{pc}) was kept ca. twice that of the anodic peak current (i_{pa}), and that the separation of the peak potentials, ΔE_p , increases with pH values. The reason for the latter was that the electrochemical behavior of the polymer deposited at the platinum electrode corresponds to a quasi-reversible signal in the pH range. According to the results obtained by Karyakin et al. [2] and Inzelt and Csaok [8], the redox couple situated at negative potentials could be ascribed to the monomer-type set of redox peaks, i.e. the electron transfer is coupled with protonation/deprotonation processes.

Besides the first redox reaction the second wave, less pronounced, also occurs at higher positive potentials (at ca. 0.15 V) in Fig. 2A. It can be seen from Fig. 2A that the second redox peak is not shifted between pH 1.0 and 4.0.

Although the second redox peak is unseen at 60 mV s^{-1} on curve 7 in Fig. 2B, it indeed appears in the solution with pH 7.0 at 250 mV s^{-1} (see curve 4 in Fig. 4B). This means that the PNR-SFCA film still has an electroactivity at pH 7.0. This property of the PNR-SFCA is better than that of normal polyaniline and PNR synthesized from strong acid solutions free of SFCA [14,38]. In view of the redox peak obtained from the solutions with pH 7.0 at 250 mV s^{-1} and pH 5.0 at 60 mV s^{-1} , it can be seen that the redox couple at ca. 0.15 V is also shifted hardly in the range of pH 5.0–7.0.

Thus, the redox peak at ca. 0.15 V is not shifted between pH 1.0 and 7.0. This means that the second redox process of the polymer is a none-proton reaction, although its peak currents decrease as pH value increases from 1.0 to 7.0. In addition, ΔE_p of the second redox peak is also a non-zero value. Taking into account the fact that the second redox peak could be attributed to the redox reaction of the polymer [2,8], we deduce that the second redox process is accompanied by doping/dedoping of anions. This is also similar to that of the redox peak of polyaniline at ca. 0.10 V [39].

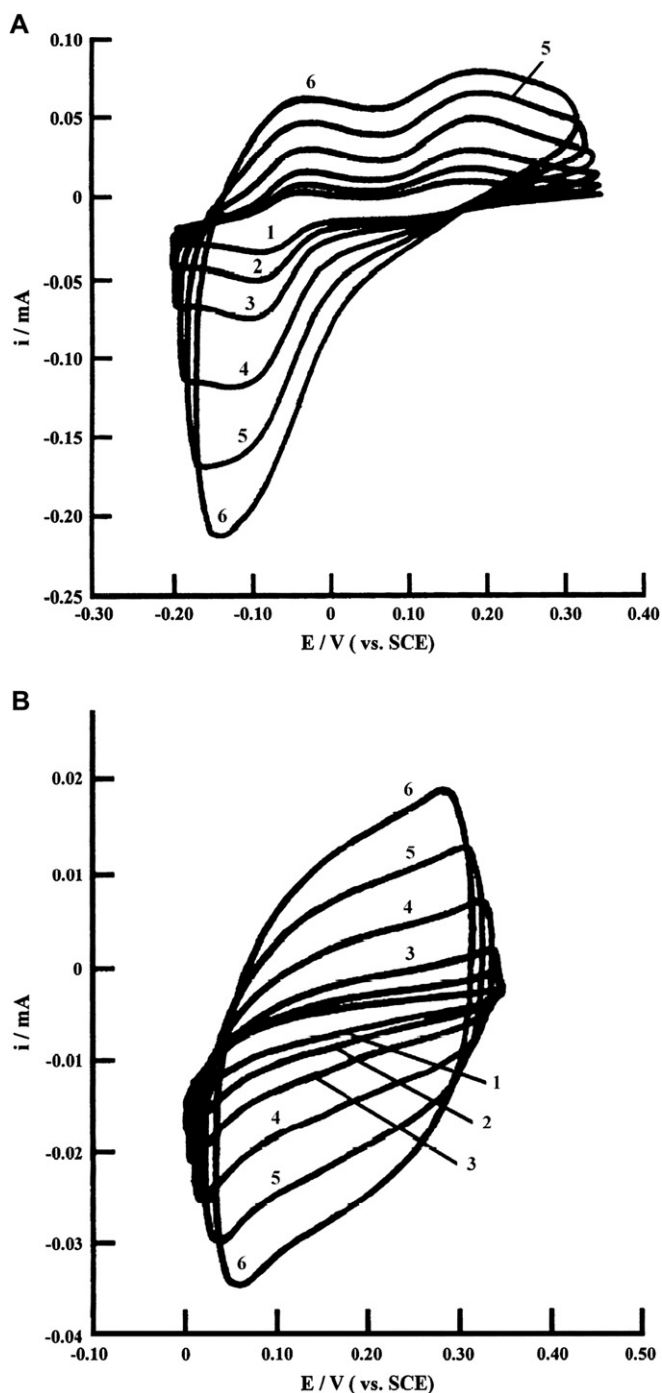


Fig. 4. Effect of potential scan rate on the cyclic voltammograms of PNR-SFCA in $0.5 \text{ mol dm}^{-3} \text{ Na}_2\text{SO}_4$ solutions with pH 1.0 (A) and 7.0 (B). Curves: (1) 25, (2) 50, (3) 100, (4) 200, (5) 400, (6) 600 mV s^{-1} .

3.3. Effect of the scan rate on the cyclic voltammograms of PNR-SFCA

Fig. 4A and B exhibits the effect of the potential scan rate on the cyclic voltammograms of PNR-SFCA in $0.5 \text{ mol dm}^{-3} \text{ Na}_2\text{SO}_4$ solutions with pH 1.0 and 7.0, respectively.

In Fig. 4A, their peak currents increase with potential scan rates, and all the peak potentials are independent of potential scan rate in the range of 25–600 mV s^{-1} . There are still two

anodic peaks and a sharp cathodic peak at 600 mV s^{-1} on curve 6 in Fig. 4A, indicating that the electrochemical reaction is still controlled by mass transfer at such a high scan rate. Based on the relationship between the potential scan rate v and the anodic (cathodic) peak current, the peak currents varied linearly with $v^{1/2}$. This again proves that the electrode reaction of PNR-SFCA is controlled by mass transfer and the PNR-SFCA still has a good ability of the charge transfer at pH 1.0. In addition, the $i-E$ curves in Fig. 4A indeed have a cathodic peak at about 0.13 V as can be seen in Fig. 2A, but it may be too weak and broad to be observed in this case.

In Fig. 4B, there is no redox couple on curve 1. This may be caused by the unstable state of PNR-SFCA. Indeed curves 3–6 show a very weak redox peak which is not shifted with increasing scan rates. This means that PNR-SFCA still has an electrochemical reversibility and a charge transfer characteristic at pH 7.0.

3.4. Visible spectra

Curves 1 and 2 in Fig. 5 show the visible spectra of dried neutral red and PNR-SFCA powders, respectively. There is a peak at 530 nm on curve 1 for the monomer. The signal of the monomer at 530 nm appears in the polymer but is shifted to 573 nm. This phenomenon is in good agreement with the fact that the wavelength of the absorption peak of a polymer is generally longer than that of the corresponding monomer, since the conjugation bond distance in the polymer is much longer than that of the monomer. The visible spectrum of PNR-SFCA obtained here is different from that of the normal PNR electrodeposited on glassy substrate since the latter is similar to the visible spectrum of the neutral red monomer [2,7,14,15].

It is well known that polyaniline in the emeraldine base state displays a typical electronic absorption peak at 570 nm which is attributed to the quinoid structure [27]. Taking into account the fact that neutral red is an aniline derivative, we expect that the chemical structure of poly(neutral red) here may be somewhat similar to that of polyaniline. Thus, the

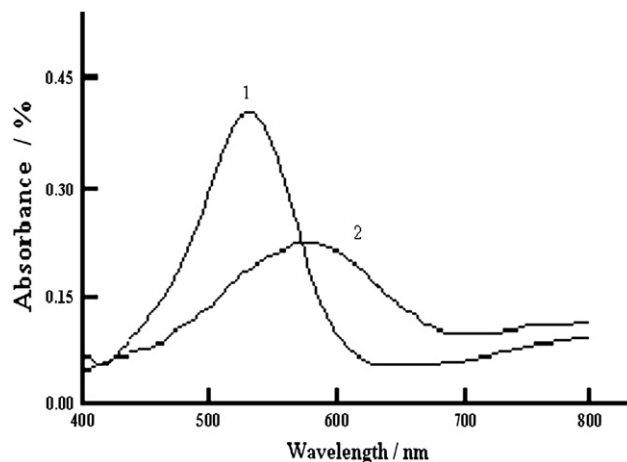


Fig. 5. Visible spectra for neutral red (1) and PNR-SFCA (2).

polymerization mechanism of neutral red is possibly similar to that of aniline, i.e. ‘head-to-tail’ coupling; amino group binds to aromatic ring. More evidence for this comes from the following IR spectra (see Section 3.5).

3.5. IR spectra

The IR spectra of neutral red (curve 1) and PNR-SFCA (curve 2), respectively, are displayed in Fig. 6. The IR spectrum of PNR-SFCA synthesized here is different from that of the poly(neutral red) (PNR) electrosynthesized on Pt from aqueous sulfuric acid solution free of SFCA since three peaks at 1505, 1190 and 730 cm^{-1} almost disappeared in curve 2 compared with the IR spectrum of PNR [15].

As shown in Fig. 6, there are 13 absorption bands at 1729 (weak), 1661 (weak), 1632 (medium), 1601 (medium), 1533 (very weak), 1446 (medium), 1407 (strong), 1382 (strong), 1327 (medium), 1250 (strong), 1234 (strong), 1076 (shoulder) and 1048 (strong) cm^{-1} , and two strong absorption bands at 2980 and 2900 cm^{-1} on curve 2 while six absorption bands at 3170 (strong), 2800 (medium), 1010 (medium), 964 (weak), 810 (strong) and 730 cm^{-1} (strong) disappear on curve 2 compared with curve 1. The two absorption peaks at 2980 and 2900 cm^{-1} on curve 2 are attributable to stretching vibrations of C–H in alkyl groups and aromatic rings. The absorption peak at 1729 cm^{-1} in polymer spectrum is attributed to the C–H vibrations in ferrocene [28,40]. The two peaks at 1661 and 1048 cm^{-1} are mainly attributed to C–H vibrations of phenazine ring and SFCA. In addition, the peak at 1661 cm^{-1} is partly attributed to carboxylic anions, indicating that SFCA was doped into the resulting polymer. Three peaks of the monomer at 1616, 1496 and 1442 cm^{-1} , which are all attributed to phenyl ring stretching vibrations, or a mixture of C=C and C=N vibrations in phenazine ring, appear in the polymer spectrum but are shifted to 1601, 1533 and 1446 cm^{-1} . The absorption peak at 1632 cm^{-1} is also attributed to the C=C vibration of aromatic rings in phenazine and ferrocene while the absorption peak at 1407 cm^{-1} is assigned to the out-of-plane C–H bending vibration of arenes from ferrocene, or a mixture of C=C and C=O vibrations from SFCA. The peak at 1234 cm^{-1} on curve 2 is attributed to the C–N vibration. The PNR-SFCA spectrum also shows two characteristic absorption peaks at 1250 cm^{-1} due to stretching vibration of SO_2 in SO_4^{2-} (sulfate) and at 1076 cm^{-1} due to stretching vibration of SO_2 in R– SO_3H (sulfonic acid) [41]. This again proves that SFCA was doped into the PNR-SFCA film since $-\text{SO}_3\text{H}$ groups doped into the resulting polymer came from SFCA. More evidence for this comes from the following XPS experiment of the PNR-SFCA (see Section 3.6).

As seen in Fig. 6, the N–H stretching vibration peaks in the monomer at 3330 and 3170 cm^{-1} were replaced by a new weak broad band at 3374 cm^{-1} for the PNR-SFCA. This new band is attributed to the N–H stretching vibrations coupled with O–H stretching vibrations of the carboxylic acid. This means that the transformation of a primary to a secondary amine and coupling occurred through the amino groups and

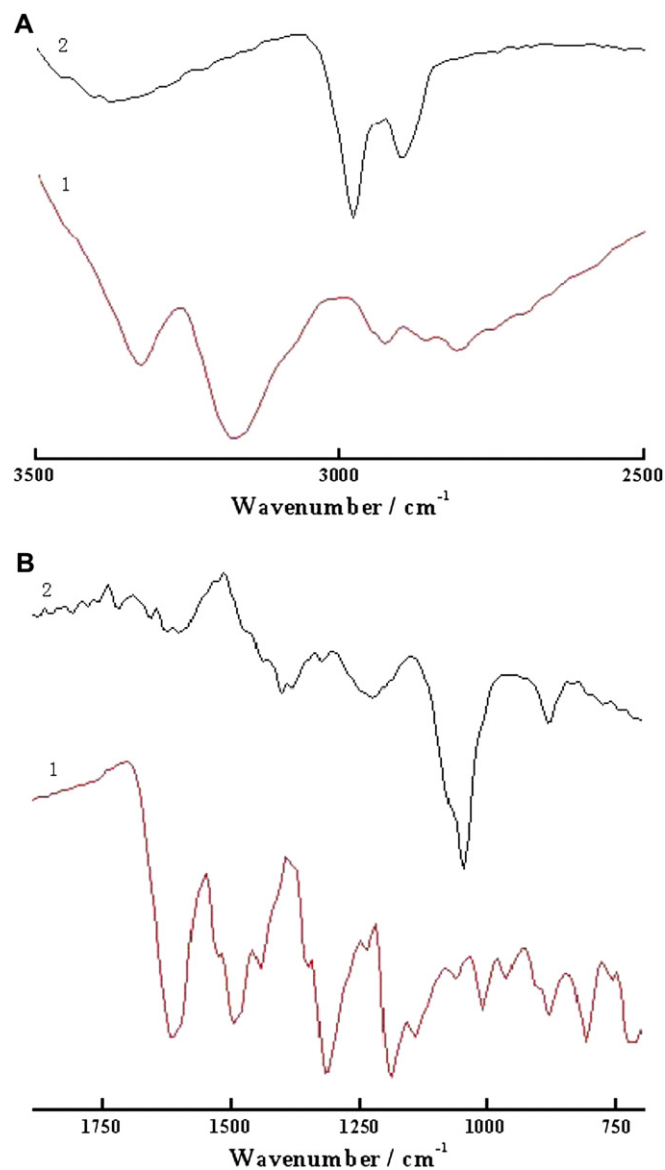


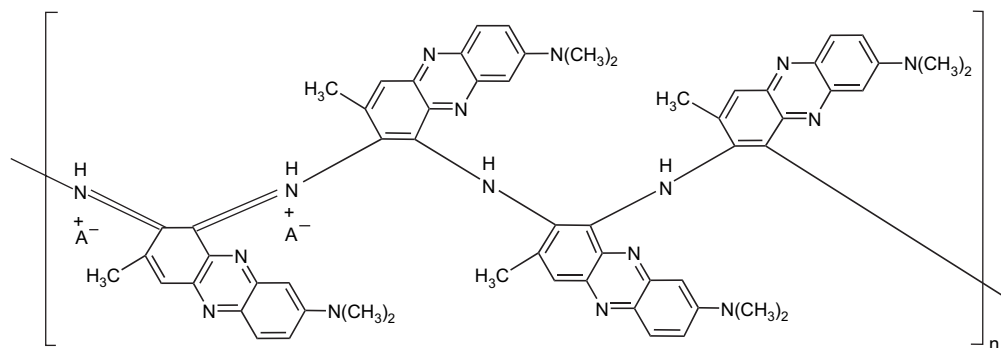
Fig. 6. IR spectra in the wave number region of 2000–4000 cm^{-1} (A) and 2000–700 cm^{-1} (B) for neutral red (1) and PNR-SFCA (2).

that the resulting polymer was also doped with SFCA (since the carboxylic acid came from SFCA). In addition, a single strong band at 880 cm^{-1} , which is attributed to out-of-plane C–H bending vibrations, appears below 900 cm^{-1} on curve 2. It is a characteristic absorption peak of a penta-substituted benzene ring [42]. Thus, the monomeric units are *ortho*-coupled since the other *ortho*-position and the *para*-position of $-\text{NH}_2$ in the neutral red monomer are occupied by $-\text{CH}_3$ and pyrazine ring, respectively.

Based on the above results and the structure of polyaniline [38], the possible chemical structure of the PNR-SFCA is shown in Scheme 2, where A^- is an anion doping the polymer film.

3.6. XPS of the PNR-SFCA

Table 1 displays the XPS experimental results of the resulting polymer film. There are C, N, S, O and Fe atoms in the



Scheme 2. Possible chemical structure of the PNR-SFCA.

polymer. The first two atoms (C and N) are expected, since they came from neutral red. Sulfur and oxygen atoms came from both sulfate ions from H_2SO_4 as the supporting electrolyte and $-\text{SO}_3\text{H}$ groups from SFCA as a protonic acid dopant in this work. In addition, oxygen atom may mainly be attributed to the oxygen and water adsorbed in the polymer as that in polyaniline detected by XPS [43,44], since the relative content of the oxygen atom is 23.7% here. Fe atom is also expected since it came from SFCA which was used as a protonic acid dopant here.

The C 1s peak in the XPS spectra of PNR-SFCA as well as normal polyaniline is split into three peaks in the binding energy range between 284 and 289 eV [45,46]. One peak with the binding energy 288.7 eV may be attributed to the carbon atom (in aromatic ring) that binds to $-\text{N}(\text{CH}_3)_2$ or the carbon atom (in carboxylic acid) that comes from SFCA, since the carbon atom is attached to an electro-negative nitrogen atom (in $-\text{N}(\text{CH}_3)_2$) or oxygen atom (in $-\text{COO}^-$), i.e. the chemical environment of the C atom is different from those of other C atoms. The N(O) atom plays a direct and indirect role in decreasing the shielding of the positive nuclear charges of C 1s by outer electrons. Thus the effective attractive force of the nucleus with regard to the core electrons of C 1s is increased, i.e. its binding energy should be higher than those of other carbon atoms in the polymer. In addition, the content of the C atoms having 288.7 eV is the lowest among the three kinds of C 1s, which is also an evidence for C 1s originating from the carbon atom (in aromatic ring) that binds to $-\text{N}(\text{CH}_3)_2$ or the carbon atom (in carboxylic acid) that comes from SFCA. In the polymer, one peak of C 1s with 286.4 eV may be originating from the carbon atom (in aromatic ring) that binds to $-\text{NH}_2$, the reason for which is similar to that

of the peak at 288.7 eV. Another peak of C 1s with 284.7 eV should be originating from C=C (in aromatic ring) and C-H (in both aromatic ring and alkyl).

Although the relative content of the Fe atom is only 0.5%, the small amount of Fe atom indicates that SFCA was doped into the resulting polymer. Furthermore, we could deduce that a ratio of SO_4^{2-} and $-\text{SO}_3\text{H}$ groups in the resulting polymer is ca. 1:2, taking into account the fact that the ratio of the Fe to sulfur atoms in SFCA is 1:1 and the semiquantitative XPS result that the relative content of the sulfur atom is only 1.6%. Since the XPS S/O ratio (0.07) is much lower than that expected for SO_4^{2-} or $-\text{SO}_3\text{H}$, indicating that oxygen atom comes partly from SO_4^{2-} and $-\text{SO}_3\text{H}$ doped in polymer film and is mainly attributed to the oxygen and water adsorbed in the polymer.

In addition, the XPS N 1s peak with binding energy of 400.0 eV is attributed to the imine ($-\text{N}=\text{C}$) and amine ($-\text{NH}-$) nitrogens [47]. Therefore, the above XPS results indicate that SO_4^{2-} and SFCA could be co-doped in the resulting polymer and coupled with the protonated nitrogen of PNR-SFCA.

3.7. SEM morphology of the PNR-SFCA film

Fig. 7A shows that the scanning electron microscopy (SEM) image of PNR-SFCA film portray curving, branching

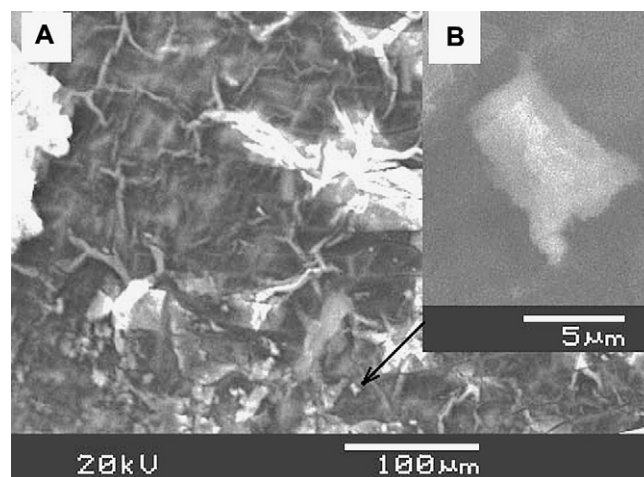


Fig. 7. SEM photographs of PNR-SFCA film.

Table 1
XPS experimental results of the PNR-SFCA film

Peak	Binding energy (eV)	Atom percentage (%)
C 1s	284.7	55.3
	286.4	10.3
	288.7	5.3
N 1s	400.0	3.3
S 2p	167.6	1.6
O 1s	532.2	23.7
Fe 2p ³	708.2	0.5

and rocky features. In addition, it can be seen from Fig. 7A that the surface of the resulting polymer partly consisted of hills and particles. Among them there is one micro-tube with ca. 4 μm in diameter and 8 μm in length (Fig. 7B). These filigree patterns are termed “topographic-types” or “geologic-types” because of their similarity to some images of Earth from space [48] or Titan taken by Huygens [49]. This indicates that there may be some similarity to the topographic structure formations of macrocosmic and microcosmic materials in Nature. Since the geologic features of Titan and Earth were likely carved by a flowing liquid, the morphology formation of the polymer may also be caused by the aqueous electrolytic solution.

In a recent paper, we reported that the SEM image of PNR is a micro-structured network [15]. It is clear that the morphology of PNR-SFCA obtained here is different from that of PNR, indicating that SFCA induces changes in the morphology of PNR film. This is in good agreement with the fact that the morphology of the conducting films has been shown to be dependent upon both the dopant anion incorporated and the conditions of polymer formation [50]. Also, this similar phenomenon of polyaniline doped with transition metals was observed [51]. Thus, SFCA may play an important role in formatting the surface structure of the PNR-SFCA film.

Besides that, since Earth surface is also caused by earth erosion and the transportation and deposition of earth, we believe the morphology of PNR-SFCA also originates from the polymer erosion and the transportation and the deposition of the polymer during the electrolysis process, taking into account the fact that there are polymer hills with a layered micro-structure in Fig. 7A.

According to the above discussions, we deduce both the flowing aqueous solution of SFCA and the sedimentation and erosion of the polymer result in the final surface micro-structure of PNR-SFCA.

4. Conclusion

Electrochemically active polymer films are formed on platinum during continuous potential cycling in sulfuric acid and SFCA solution containing neutral red and the electrochemical characteristics of the resulting polymer are somewhat similar to those of normal polyaniline film but are better than the latter. The redox reaction of the resulting polymer at more negative potentials contains a relatively simple $1e^-$, $2H^+$ process. In addition, the potentials of the other redox couple change hardly from pH 1.0 to 7.0, i.e. the redox process of the resulting polymer at higher positive potentials is a non-proton reaction. However, the PNR-SFCA film still has an electrochemical activity in solutions at pH 7.0 at 250 mV s^{-1} . The effect of the scan rate on the cyclic voltammograms of the PNR-SFCA in aqueous solutions with pH 1.0 and 7.0 reveals that the polymer in both solutions has an electrochemical reversibility and a charge transfer characteristic and the electrode reaction rate of the polymer is controlled by mass diffusion. The SEM morphology of PNR-SFCA film is a geologic-type surface structure, very similar to Earth

and Titan. This reason may be both due to the flowing aqueous solution containing SFCA and the deposition and erosion of the polymer. According to the UV–vis and IR spectra, a possible chemical structure of the corresponding polymer is proposed here, i.e. the polymer is formed *via* C–N couplings. IR spectra and XPS data also prove that both SFCA and SO_4^{2-} are co-dopants of the resulting polymer. However, the electrosynthesis mechanism and chemical and surface structures of the resulting polymer are rather complicated, thus a further study on them is required. Its applications are also to be investigated in detail.

Acknowledgements

This work was supported by the Social Development Foundation of Zhenjiang City (no. SH2006076). Thanks are due to Professor Mingrong Ji (Center of Physics and Chemistry, University of Science and Technology of China) for his help in the XPS determination.

References

- [1] Puskas Z, Inzelt G. *Electrochim Acta* 2005;50(7–8):1481–90.
- [2] Karyakin AA, Karyakina EE, Schmidt HL. *Electroanalysis* 1999;11(3):149–55.
- [3] Karyakin AA, Ivanova YN, Karyakina EE. *Electrochem Commun* 2003;5(8):677–80.
- [4] Lyons MEG, Fay HG, Mitchel C, MacCormac DE. *Anal Chem Symp Ser* 1986;25:285.
- [5] Benito D, Gabrielli C, Garcia-Jareno JJ, Keddad M, Perrot H, Vicente F. *Electrochim Acta* 2003;48(27):4039–48.
- [6] Vicente F, Garcia-Jareno JJ, Benito D, Agrisuelas J. *J New Mater Electrochem Syst* 2003;6:267–74.
- [7] Chen SM, Lin KC. *J Electroanal Chem* 2001;511(1–2):101–14.
- [8] Inzelt G, Cshok E. *Electroanalysis* 1999;11(10–11):744–8.
- [9] Kertesz V, Bacskai J, Inzelt G. *Electrochim Acta* 1996;41(18):2877–81.
- [10] Benito D, Gabrielli C, Garcia-Jareno JJ, Keddad M, Perrot H, Vicente F. *Electrochem Commun* 2002;4(8):613–9.
- [11] Qu FL, Yang MH, Chen JW, Shen GL, Yu RQ. *Anal Lett* 2006;39(9):1785–99.
- [12] Ghica ME, Brett CMA. *Anal Lett* 2006;39(8):1527–42.
- [13] Karyakin AA, Bobrova OA, Karyakina EE. *J Electroanal Chem* 1995;399(1–2):179–84.
- [14] Chen CX, Zhu HP. *Bull Electrochem* 2002;18(6):247–53.
- [15] Chen CX, Gao YH. *Electrochim Acta* 2007;52(9):3143–8.
- [16] Hammache H, Makhloufi L, Saidani B. *Synth Met* 2001;123(3):515–22.
- [17] Bennett MD, Leo DJ, Wilkes GL, Beyer FL, Pechar TW. *Polymer* 2006;47(19):6782–96.
- [18] Li GT, Bhosale S, Tao SY, Guo RR, Bhosale S, Li FT, et al. *Polymer* 2005;46(14):5299–307.
- [19] Murray RW. *Electroanal Chem* 1983;13:191–368.
- [20] Daum P, Murry RW. *J Phys Chem* 1981;85(4):389–96.
- [21] Daum P, Lenhard JR, Rolison D, Murry RW. *J Am Chem Soc* 1980;102(14):4649–53.
- [22] Inzelt G. *Electrochim Acta* 1989;34(2):83–91.
- [23] Nishihara H, Shimano Y, Aramaki K. *J Phys Chem* 1987;91:2918–21.
- [24] Xue XJ, Wang L, Wang JJ, Chen T. *J Phys Chem B* 2004;108(18):5627–33.
- [25] Chen T, Wang L, Jiang GH, Wang JJ, Dong XC, Wang XJ, et al. *J Phys Chem B* 2005;109(10):4624–30.
- [26] Pourmaghi-Azar MH, Ojani R. *J Solid State Electrochem* 1999;3(7–8):392–6.
- [27] Yamamoto K, Yamada M, Nishiumi T. *Polym Adv Technol* 2000;11(8–12):710–5.

- [28] Shan D, Mu SL. *Synth Met* 2002;126(2–3):225–32.
- [29] Mu SL, Kan JQ. *Synth Met* 2002;132(1):29–33.
- [30] Mu SL. *Synth Met* 2003;139(2):287–94.
- [31] Mu SL, Yang YF, Tan ZA. *Acta Phys-Chim Sin* 2003;19(7):588–92.
- [32] Mu SL. *Synth Met* 2004;143(3):259–68.
- [33] Yang YF, Mu SL. *Biosens Bioelectron* 2005;21(1):74–8.
- [34] Mu SL. *Electrochim Acta* 2006;51(17):3434–40.
- [35] Li X, Sun C, Wei ZB. *Synth Met* 2005;155(1):45–50.
- [36] Li X, Sun C, Zhou F. *J Anal Chem* 2006;61(9):896–901.
- [37] Ndamanisha JC, Wang H, Guo LP. *Chem Res Chin Univ* 2005;21(4):431–5.
- [38] Huang WS, Humphrey BD, MacDiarmid AG. *J Chem Soc Faraday Trans I* 1986;82:2385–400.
- [39] MacDiarmid AG, Chiang JC, Richter AG, Epstein AJ. *Synth Met* 1987;18(1–3):285–90.
- [40] Knox GR, Pauson PL. *J Chem Soc* 1958;12:692–6.
- [41] Inagaki N, Tasaka S, Chengfei Z. *Polym Bull* 1991;26(2):187–91.
- [42] Nakanishi K, Solomon PH. *Infrared absorption spectroscopy*. 2nd ed. San Francisco: Holden-Day; 1977 [chapter 2].
- [43] Shan D, Mu SL, Mao BW, Li YF. *Chin J Polym Sci* 2001;19(5):483–92.
- [44] Snauwaert Ph, Lazzaroni R, Riga J, Verbist JJ. *Synth Met* 1986;16(2):245–55.
- [45] Kang ET, Neoh KG, Tan KL. *Surf Interface Anal* 1993;20(10):833–40.
- [46] Wang HY, Mu SL. *Sens Actuators B* 1999;56(1–2):22–30.
- [47] Fusalba F, Belanger D. *J Phys Chem B* 1999;103(42):9044–54.
- [48] http://veimages.gsfc.nasa.gov/457/PIA01794_md.jpg
- [49] Alpert M. *Sci Am* 2005;292(4):11–2.
- [50] Warren LF, Walker JA, Anderson DP, Rhodes CG, Buckley LJ. *J Electrochem Soc* 1989;136(8):2286–95.
- [51] Dimitriev OP. *Synth Met* 2004;142(1–3):299–303.